World Academy of Science, Engineering and Technology
International Journal of Physical and Mathematical Sciences
Vol:9, No:11, 2015

A Coupled Model for Two-Phase Simulation of a Heavy Water Pressure Vessel Reactor

Damian Ramajo, Santiago Corzo, Norberto Nigro

Abstract—A Multi-dimensional computational fluid dynamics (CFD) two-phase model was developed with the aim to simulate the in-core coolant circuit of a pressurized heavy water reactor (PHWR) of a commercial nuclear power plant (NPP). Due to the fact that this PHWR is a Reactor Pressure Vessel type (RPV), three-dimensional (3D) detailed modelling of the large reservoirs of the RPV (the upper and lower plenums and the downcomer) were coupled with an in-house finite volume one-dimensional (1D) code in order to model the 451 coolant channels housing the nuclear fuel. Regarding the 1D code, suitable empirical correlations for taking into account the in-channel distributed (friction losses) and concentrated (spacer grids, inlet and outlet throttles) pressure losses were used. A local power distribution at each one of the coolant channels was also taken into account. The heat transfer between the coolant and the surrounding moderator was accurately calculated using a two-dimensional theoretical model. The implementation of subcooled boiling and condensation models in the 1D code along with the use of functions for representing the thermal and dynamic properties of the coolant and moderator (heavy water) allow to have estimations of the in-core steam generation under nominal flow conditions for a generic fission power distribution. The in-core mass flow distribution results for steady state nominal conditions are in agreement with the expected from design, thus getting a first assessment of the coupled 1/3D model. Results for nominal condition were compared with those obtained with a previous 1/3D single-phase model getting more realistic temperature patterns, also allowing visualize low values of void fraction inside the upper plenum. It must be mentioned that the current results were obtained by imposing prescribed fission power functions from literature. Therefore, results are showed with the aim of point out the potentiality of the developed model.

Keywords—CFD, PHWR, Thermo-hydraulic, Two-phase flow.

I. Introduction

THE recently started nuclear power plant (NPP) Atucha II, is a Pressurized Heavy Water Reactor (PHWR) with a thermal power of 2160 MWt and electric power of 745 MWe. Different from the pressure tube type CANDU reactors, Atucha II is a pressure vessel reactor. The core has a vertical configuration housing 451 cooling channels (CC) housed in the moderator tank. Coolant is pumped at high pressure from the lower-plenum to the upper-plenum. The fuel bundles are composed by a set of 37 fuel rods of 5.3 m of active length. A set of 13 spacer grids strengthen and lining up the fuel assembly. The CCs are arranged in a 272 mm trigonal lattice pitch within the moderator tank. Atucha II employs a fuel composed of natural uranium. Deutered water (D_2O), commonly named Heavy Water (HW) is used for cooling and moderation purposes.

Ramajo, Corzo and Nigro are from the Research Center for Computational Methods CIMEC (CONICET-UNL), Santa Fe, Argentina (e-mail: dramajo@santafe-conicet.gov.ar).

A 3D drawing of the coolant circuit of Atucha II is shown in Fig. 1. The two pair of hot and cold legs are placed diametrically opposed in the RPV. In each one of the two loops the hot coolant flows through the hot leg from the RPV to the steam generator. After that, the cold coolant flows to the pump, returning to the RPV through the cold leg.

Fig. 1 Primary circuit of Atucha II

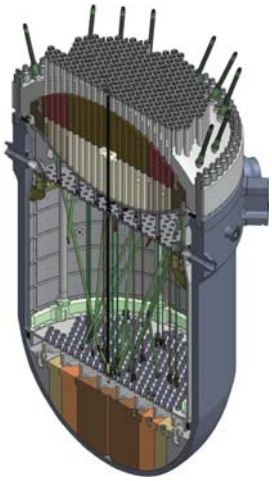

Fig. 2 Cross sectional cut view of the RPV (courtesy of [1])

The coolant circuit inside the RPV is composed of two main plenums; the cold one accounting for the annular downcomer and the lower plenum and the hot one corresponding to the upper plenum. These two large reservoirs are mainly connected through the CCs.

The coolant enters to the RPV through the two cold legs and travels down towards to the lower plenum through the

downcomer which is bounded by the RPV outer wall and the moderator tank. The lower plenum has a flow distributor composed of rhomboidal cells housing the CC inlet nozzles. Inside the CCs the coolant extracts the fission heat from the fuel assemblies and then it leaves the CCs through vertical slots placed at the end of the CCs and housed in the upper plenum. Then, the coolant from all the CCs is mixed in the upper plenum and leaves it through the two hot leg nozzles. Fig. 2 shows a cross section view of the RPV.

The upper plenum has a convex ellipsoidal shape housing 9 hafnium, 9 steel control rods and 4 boric fast injection lances. Moreover, the upper plenum is also crossed by the CCs and the moderator inlet and outlet ducts. All these components affect the flow and the thermal distribution in the upper plenum. In Fig. 2 the coloured solids above the upper and below the lower plenum are the filling bodies, which serve to reduce the coolant inventory while doing thermal dumping under transients. Only a small fraction of the coolant flows through a bypass without pass through the CCs. This bypass represents less than 3% of the total coolant flow and is used for cooling the filling bodies.

The 451 CCs are grouped in 5 hydraulic zones (HZ) with different Mass Flow Rate (MFR) following the fission radial power. This in-core flow distribution is produced by flow restrictions placed at the CC inlets. Fig. 3 shows the HZ distribution. HZ 5 is the main one, containing 253 of the 451 CCs with around 70% of the total coolant flow.

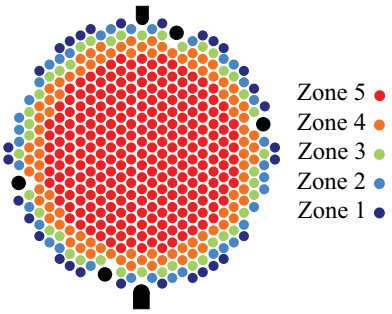

Fig. 3 Hydraulic zones of the core

During the fuel life cycle each fuel assembly is continuously changed from one CC to another CC in order to control the burnup and the fuel efficiency. The refueling process is carry on while the reactor is in-power operation [1]. The burnup distribution caused by the refueling strategy produces a radial power pattern along with the typical sinusoidal axial power pattern [2]. The central CCs release around three times more heat power than periphery CCs. Consequently, the in-core flow distribution promoted by the inlet flow restrictions at the CCs must be accurately designed to avoid thermal stratification at the upper plenum and noticeable void generation at the central channels.

The only one similar NPP is the predecessor Atucha I. Therefore, Atucha I and II are one of a kind NPP around the world. Atucha I is in operation since 1974 and valuable experience has been gained. However, Atucha II is two times larger, thus resulting in a technological challenge. Detailed explanation about this NPP can be consulted in [3].

Regarding the use of multidimensional CFD couple models, a recent work [4] dealt with the coupling of the CFD multi-physics software Fluent® and the system nuclear code ATHLET. Another contributions around coupling strategies commonly involve the use of the RELAP code [5].

The present work also proposed a multi-dimensional (1/3D) two-phase approach coupling 3D domains (upper plenum, lower plenum and downcomer) with an in-house 1D code specially formulated for modelling the pressure drop and heat and mass transfer in the CCs. This model deal with a detailed description of the coolant circuit of the whole RPV. This work is the third step in the way to develop a transient, multi-domain and multi-phase model of the reactor. It started with a 0/3D single-phase model [6], which was enhanced by incorporating 1D single-phase modelling of the CCs [7] until reach the current multiphase version. However, the model is still limited to the RPV of the NPP.

II. Computational Mdel

The coupling was achieved by the use of a novel strategy of sink/source points (SSPs) developed and assessed for the previous model versions [6], [7]. In this, the lower end of each CC (that is the inlet under normal conditions) is represented by a SSP located at the 3D lower plenum domain. Similarly, the upper end of each CC is represented by other SSP located at the 3D upper plenum domain. Fig. 4 shows an scheme of the coupling. The colours sketch the cold (blue) and hot (red) coolant while it circulates through the RPV.

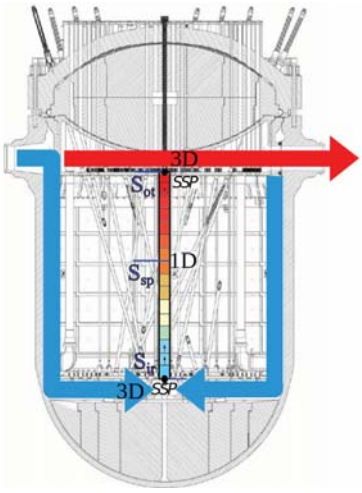

Fig. 4 Scheme displaying the coupling methodology

The information collected by the SSP pair (representing one CC) from the 3D domains becomes the inlet/outlet boundary condition for modelling the 1D CC. At the same time, the CCs results are used to feedback to the 3D domains through the mass (SS), momentum (SM) and energy (SE) source terms at the right hand side of the transport equations.

The 1D code was implemented in Fortran 90. The code is called in run time (at the beginning of each iteration of the 3D model) receiving the current flow conditions (pressure, temperature and void fraction) from the upper and lower

SSPs. Then, it calculates the requested variables (mass flow rate, temperature, void fraction and mean outlet velocity) and returns the results to the 3D solver. The coupling is done in a partitioned way, which is similar to the called loose coupling method but with extra inner iterations that forces the solution to converge in a similar way to a strong coupling method.

The 3D domain is made from the assembly of two isolated domains which are joined only through the SSPs. The upper domain contains a short part of the hot legs and the upper plenum housing the 22 guideline tubes for the control and shut down system rods, the 4 vertical moderator inlets and the 2 elbow moderator outlets. The lower domain is composed of a short part of the cold legs, the downcomer and the lower plenum housing the rhomboidal flow distributor. The fission power transferred to the coolant was imposing by taking into account an axial power distribution different for each hydraulic zone for a given burnup configuration. Of course, this is a rough approach to be carefully revised if accurate results for Atucha II want to be found.

The heat transferred from the CCs to the moderator tank represents a significant heat loss for the 1D code. Therefore it was accurately estimated in a previous work [8] by coupling the 1D code with a 3D model of the moderator tank.

The discretization of the 3D model (upper and lower plenums) demanded 9.128.118 cells (8.819.511 tetrahedrons, 3.302 pyramids and 305.305 wedges). Besides, each CC was discretized with 50 1D cells.

III. Mathematical Formulation

3D transport equations for incompressible two-phase flow have been extensively reported in bibliography and thay can also be consulted in [9]. Regarding the 1D code, in order to reproduce the significant density changes caused by the temperature variations, a conservative pseudo-compressible formulation was implemented. A cell-centered (collocated) Finite Volume Method (FVM) [10] was chosen to solve the 1D transport equations. The algorithm used is showed in Fig. 6.

In 1D formulation the mass transport equation takes the following form:

$$\frac{\partial(\alpha_1\rho_1)}{\partial t}+\frac{\partial}{\partial x}(\alpha_1\rho_1\mathbf{U_1})=\Gamma_{1,2}-\Gamma_{2,1} \quad (1)$$

$$\frac{\partial(\alpha_2\rho_2)}{\partial t}+\frac{\partial}{\partial x}(\alpha_2\rho_2\mathbf{U_2})=\Gamma_{2,1}-\Gamma_{1,2} \quad (2)$$

where α_1 and α_2 denote the volume fraction of phases 1 and 2 respectively (note that $\alpha_1+\alpha_2=1$). ρ_1 and ρ_2 are the densities of the fluids, $\mathbf{U_1}$ and $\mathbf{U_2}$ are the phase velocities. Finally, T$\Gamma_{1,2}$ and $\Gamma_{2,1}$ are the evaporation and condensation rates respectively.

The momentum equations can be written as:

$$\frac{\partial(\alpha_1\rho_1\mathbf{U_1})}{\partial t}+\frac{\partial}{\partial x}(\alpha_1\rho_1\mathbf{U_1}\mathbf{U_1})=-\alpha_1\frac{\partial p}{\partial x}+\alpha_1\rho_1\mathbf{g}+\frac{1}{2}\frac{\rho_1}{D_h}\lambda_1{\mathbf{U_1}}^2+\frac{1}{2}\frac{\rho_1}{\Delta x}\zeta_1{\mathbf{U_1}}^2+\mathbf{M_{1,2}}+(\Gamma_{1,2}\mathbf{U_1}-\Gamma_{2,1}\mathbf{U_2}) \quad (3)$$

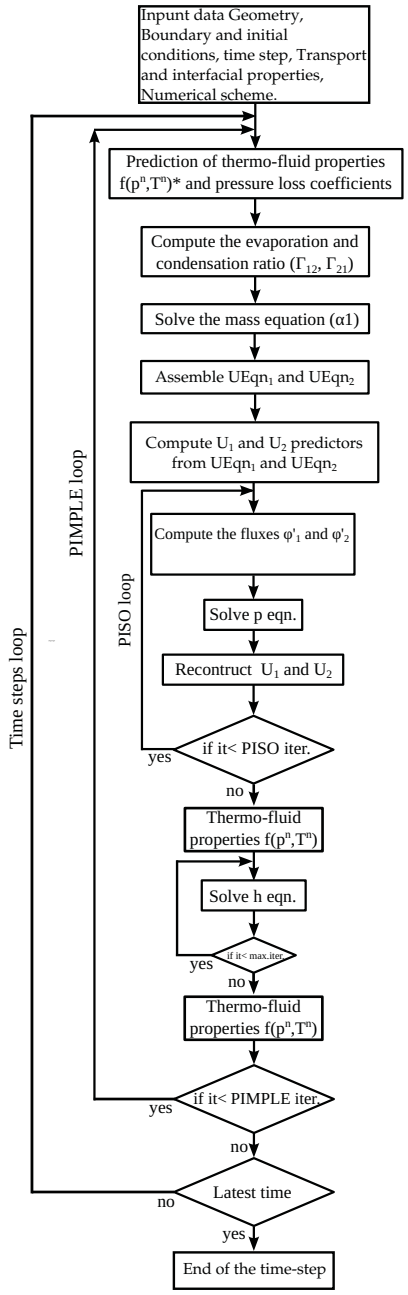

Fig. 5 Algorithm for 1D code solver.

$$\frac{\partial(\alpha_2\rho_2\mathbf{U_2})}{\partial t}+\frac{\partial}{\partial x}(\alpha_2\rho_2\mathbf{U_2}\mathbf{U_2})=-\alpha_2\frac{\partial p}{\partial x}+\alpha_2\rho_2\mathbf{g}+\frac{1}{2}\frac{\rho_2}{D_h}\lambda_2{\mathbf{U_2}}^2+\frac{1}{2}\frac{\rho_2}{\Delta x}\zeta_2{\mathbf{U_2}}^2+\mathbf{M_{2,1}}+(\Gamma_{2,1}\mathbf{U_2}-\Gamma_{1,2}\mathbf{U_1}) \quad (4)$$

Here, p is the pressure, $\mathbf{g}$ is te gravitational acceleration and $\mathbf{M_{1,2}}$, $\mathbf{M_{2,1}}$ are the interface forces per unit volume (where $\mathbf{M_{1,2}}=-\mathbf{M_{2,1}}$). In (3) and (4), the third and fourth terms on the right hand side represent the pressure drop caused by the wall friction and by form losses.

The wall diffusion effects and the form pressure losses are modelled using the Darcy-Weisbach equation, making use of empirical correlations from literature, experimental data from technical reports and previous CFD simulations:

$$\left(\frac{dp}{dx}\right)_{\gamma} = \frac{1}{2}\lambda_{\gamma}\rho_{\gamma}U_{\gamma}^{2}\left(\frac{1}{D_h}\right) \tag{5}$$

where D_h is the hydraulic diameter and λ_γ is the Darcy friction factor or the form coefficient. The single-phase estimations for the pressure drop are corrected for two-phase flow using the Lockhard-Martinelli approach.

Due to the gas phase (steam) is considered as saturated, only the thermal equation for the liquid phase is solved in terms of the specific thermal enthalpy h_1. It is written as:

$$\begin{aligned}\frac{\partial}{\partial t}(\alpha_1\rho_1 h_1) + \frac{\partial}{\partial x}(\alpha_1\rho_1 h_1 \mathbf{U_1}) - \alpha_1\frac{\partial p}{\partial x} \\ = -\nabla\cdot(\alpha_1\mathbf{q_1}) + h_{1,2}(T_2 - T_1) + \\ (\Gamma_{1,2}h_1 - \Gamma_{2,1}h_2) + A_{w,1}q_w\end{aligned} \tag{6}$$

where $\mathbf{q_1}$ is the heat flux transferred by conduction and defined by the Fourier law. $h_{1,2}(T_2 - T_1)$ represents the heat transferred between phases, $(\Gamma_{1,2}h_1 - \Gamma_{2,1}h_2)$ is the energy transferred by mass change during evaporation and condensation and q_w is the wall heat transfer. As noted, the energy dissipation/production by viscous work is neglected.

A. Heat Transfer Models

Heat transfer in 1D domains were accomplished by using wall heat flux partitioning model. To obtain the wall evaporation in subcooled conditions the Lahey model [11] seems to be the better choice. Regarding condensation, the model from Unal [12] was choice. Then, the wall evaporation rate is calculated as:

$$\Gamma_{1,2} = \frac{q_w\left[1 - \left(\frac{h_{l,s}-h_l}{h_{l,s}-h_{OSV}}\right)\right]}{h_{lg}}\frac{1}{(1+\epsilon)} \tag{7}$$

where $h_{l,s}$ is the saturated liquid enthalpy, h_{lg} is the latent heat and h_{OSV} the liquid enthalpy at the Onset of Significant Void (OSV). This point was assumed as the location where net void fraction begin to exist. The empirical parameter ϵ is the agitation ratio and was computed using the Rouhani et. al. correlation [14]. Unal [13] proposed that the T_{OSV} can be found by the following expression:

$$\frac{h_{fc0}(T_{l,s} - T_{OSV})}{q_w} = a \tag{8}$$

where $a = 0.24$ for $U_l \geq 0.45m/s$ and $a = 0.11$ for $U_l < 0.45m/s$.

Condensation mass flow rate $\Gamma_{2,1}$ in the bulk is computed by an interface heat transfer coefficient:

$$\Gamma_{2,1} = \frac{h_{if}A_{if}(T_{l,s} - T_l)}{h_{lg}} \tag{9}$$

where, h_{if} is the interface heat transfer coefficient and A_{if} the interfacial area. Several authors have proposed expressions for computing these two variables. In this work (and also in RELAP5) a "total heat transfer coefficient" $H_{if} = h_{if}A_{if}$ is computed by a modified Unal correlation [12], which for bubbly regime takes the following form:

$$H_{if} = h_{if}A_{if} = \frac{F3F5\alpha_{bub}C\Phi h_{fg}\rho_f\rho_g}{(\rho_f - \rho_g)} \tag{10}$$

where α_{bub} is the steam void fraction in bubbly regime. $F3$, $F5$, C and Φ represent model coefficients. In Fig. 6 are summarized the models employed in the 1D code. Details about the implementation can be found in [9].

Evaporation model		Lahey
	Evaporation ratio	Eqn. 7
	OSV point	Unal (eqn. 8)
Condensation model		Unal
	Condensation ratio	Eqn. 9
	Heat tranfer coefficient	Modified Unal correlation (eqn. 10)
Interfacial forces	Drag force	Ishii-Zuber
	Virtual mass force	-
Frictional pressure drop	Single-phase coef.	Colebrook-White
	Two-phase correction	Lockhard-Martinelli
Form pressure drop	Inlet restrictors	Experimental data
	Spacers	3D CFD results.
	Outlet throttle	3D CFD results.
Fluid properties	Heavy water (ρ, μ, Cp)	Polynomial interpolation functions.

Fig. 6 Algorithm for 1D code solver

IV. Results and Discussion

Numerical results of the steady state solutions describing the overall flow behaviour of the RPV are presented in this section. The results helped to evaluate the capabilities of the developed computational models, which combines the coupling strategy (SSPs) with the pseudo-compressible formulation for the 1D CC modeling. These results allowed to calculate some in-core features such as the MFR in each CC for comparing with the expected from design.

Fig. 7 compares the MFR and coolant temperature at the CC outlets from the 0/3D Single-Phase [8], the 1/3D Single-Phase [7] and the 1/3D Two-Phase [9] versions. The MFR for each CC is shown at the left plot. As noted, for the core center (HZ 5) the MFR from the 1/3D versions are less than for the previous 0D version. On the other hand, the MFR estimation at the peripheral CCs becomes greater for the 1/3D versions. The MFR expected from design is also included for comparison.

Fig. 8 shows the flow distribution inside the downcomer and the both plenums. For confidential reasons, the temperature scales in all the graphics must have been removed. The blue streamlines correspond to the inlet flow and the red ones to the outlet flow. Due to the shape of the joint between the cold legs and the downcomer, the entering coolant impacts with

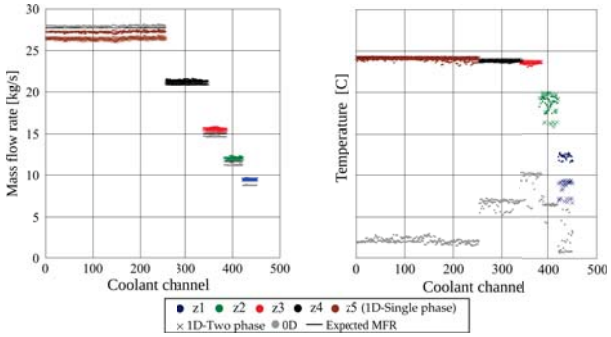

Fig. 7 1D results for CCs: 1 (HZ:5), 254 (HZ:4), 339 (HZ:3), 383 (HZ:2) and 422 (HZ:1)

the moderator tank wall and flows with less restriction in the lateral direction than in the bottom one. On the other hand, the outlet flow (red lines) is shared almost homogeneously between both hot legs.

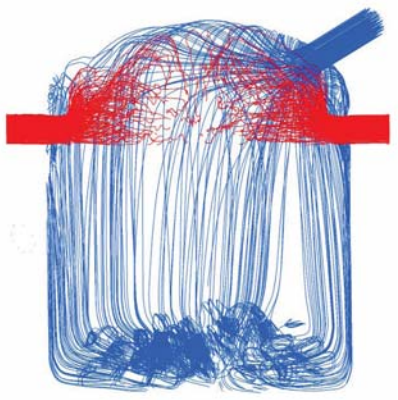

Fig. 8 Streamlines in the downcomer, lower plenum and upper plenum (blue lines: inlet flow, red lines: outlet flow)

Fig. 9 shows the liquid temperature profiles over an horizontal plane cutting the upper plenum at the height of the upper SSPs. Note that the thermal pattern seems to follow the HZ distribution. As expected, the maximum temperature is achieved in the central zone. On the other hand, the temperature near to the periphery wall is greater than the temperature of the coolant coming from the periphery CCs. This phenomenon is caused by a hot stream coming from the top of the upper plenum as can be noted in Fig. 10. In this figure is shown the velocity pattern in several vertical planes in the upper plenum. The flow is characterized by several vortex structures. The picture shows that the more heated fluid flows from the central CCs towards to the periphery and downs close to the wall. The effect is more clearly appreciated over the plane 1.

Fig. 11 gives insight into the velocity and temperature profiles over a vertical plane cutting the upper plenum and the hot legs. Note that the fluid strongly accelerates around the hot leg mouths. Mixing becomes intense because on the presence of the control rod guidelines and the CC tubes above

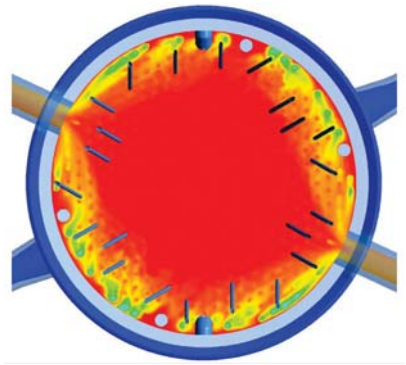

Fig. 9 Liquid temperature over a horizontal plane cutting the SSPs

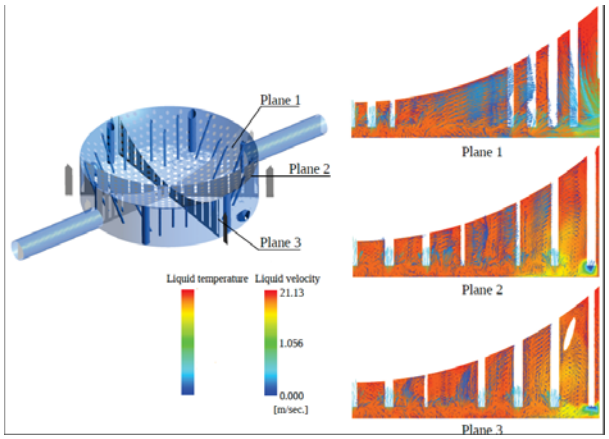

Fig. 10 Liquid velocity vectors and temperature distribution in several vertical planes in the upper plenum.

the SSPs but mainly due to the velocity of the coolant leaving the SSPs.

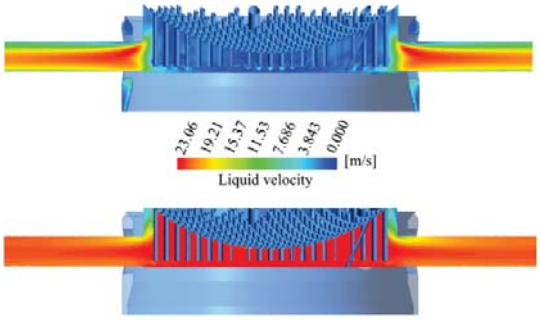

Fig. 11 Velocity and temperature profiles over a plane cutting the hot legs.

The temperature across the vertical plane cutting the hot legs seems to be slight stratified but in really the differences are less than 0.6°C. Thermal stratification in the hot legs is negligible and occurs due to the contributions of the peripheral CCs for which the coolant heating is less intense and their flow is easily conducted to the hot legs. As an example, in a recent

work, Chiang et al. [15] reported thermal stratifications more than 15°C for a PWR.

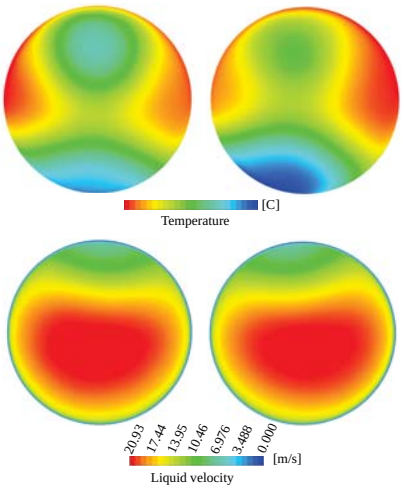

Fig. 12 Liquid temperature (upper), liquid velocity (bottom) profiles at the hot leg outlets

V. Conclusion

The 1/3D two-phase model allowed an estimation of the pressure drop, the coolant heating and the evaporation along each one of the 451 CCs. The compressible formulation offers a suitable approach to the density variations and its effect over velocity in steady state solutions.

In view of the 1/3D results, it can be concluded that this current model version is in good agreement with the expected from design for nominal operation conditions. It should be remarked the useful information provided about the in-core mass flow distribution in the RPV.

The results from the current 1/3D version are closer to the nominal data than the two previous versions. Regarding about the in-channel pressure drop, the two-phase results are in agreement with the ones obtained from the earlier single-phase model. It is easy justified by the very low void fraction estimated by the model for nominal conditions.

Acknowledgment

Authors want to thank to Universidad Nacional del Litoral (CAI+D 2011 PJ 500 201101 00015 and CAI+D PI 501 201101 00435) and CONICET (PIP 112 201101 00331). Also, they want to thank to Autoridad Regulatoria Nuclear (ARN) for financial support.

References

[1] Adorni, M., and Del Nevo, A., and DÁuria, Francesco and Mazzantini, OscarA procedure to address the fuel rod failures during LB-LOCA transient in Atucha-2 NPP

[2] O. Mazzantini, M. Schivo,J. Csare, R. Garbero, M. Rivero and G. Theler. A coupled calculation suite for atucha ii operational transients analysis, *Science and Technology of Nuclear Installations*, 2010.

[3] M. Pecchia, Application of MCNP for Predicting Power Excursion During LOCA in Atucha-2 PHWR, PhD Thesis, Univ. di Pisa, 2012.

[4] L. Vyskocil and J. Macek, Coupling CFD code with system code and neutron kinetic code, *Nuclear Engineering and Design*, Vol 279, 210-218, 2014.

[5] D. Aumiller, E. Tomlinson, W. Weaver, An integrated relap5-3d and multiphase CFD code system utilizing a semi-implicit coupling technique. *Nuclear engineering and design*, 216(1), 77-87, 2002.

[6] D. Ramajo, S. Corzo,N. Schiliuk and N. Nigro. 3d modeling of the primary circuit in the reactor pressure vessel of a phwr, *Nuclear Engineering and Design*, Vol 265, 356-365, 2013.

[7] S. Corzo,D. Ramajo and N. Nigro. 1/3d modeling of the core coolant circuit of a phwr nuclear power plant, *Annals of Nuclear Energy*, Vol 83, 386-397, 2015.

[8] D. Ramajo, S. Corzo, N. Schiliuk, A. Lazarte and N. Nigro. CFD Modeling of the Moderator Tank of a PHWR Nuclear Power Plant, *ENIEF 2014*, Vol XXXIII, 2913-2926, 2014.

[9] S. Corzo. Assessment of Nuclear Power Reactor using Computational Fluid Dynamics., PhD Thesis. Univ. Nac. del Litoral, 2015.

[10] J. Ferziger and M. Peric, *Comp. Methods for Fluid Dynamics*, Vol 3, Springer, berlin, 1999.

[11] R. Lahey. A mechanistic subcooled boiling model. Proceedings of the *6th International Heat Transfer Conference*, vol. 1, pp. 293-297, 1978.

[12] H. Unal. Maximum bubble diameter, maximum bubble-growth time and bubble-growth rate during the subcooled nucleate flow boiling of water up to 17.7mn/sq m. *International Journal of Heat and Mass Transfer 19*, 643-649, 1976.

[13] H. Unal. Determination of the initial point of net vapor generation in flow boiling systems. *International Journal of Heat and Mass Transfer* 18(9), 1095-1099, 1975.

[14] S. Rouhani, E. Axelsson. Calculation of void volume fraction in the subcooled and quality boiling regions. *International Journal of Heat and Mass Transfer*, 13(2), 383-393, 1970.

[15] J. Chiang, B. Pei, F. Tsai, Pressurized water reactor (PWR) hot-leg streaming: Part 1: Computational fluid dynamics (C) simulations. *Nuclear Engineering and Design* 241(5), 1768-1775, 2011.